Evaluation of the Non-destructive Character of the Stiffness Damage Test for Damage Assessment of Concrete Structures Affected by Alkali-Silica Reaction Using Acoustic Emission

Patrick Holthuizen(✉), Yubao Zhou, Branko Šavija, and Oğuzhan Çopuroğlu

Faculty of Civil Engineering and Geosciences, Delft University of Technology, Delft, The Netherlands
P.E.Holthuizen@tudelft.nl

Abstract. The Stiffness Damage Test (SDT), a cyclic test in compression, is considered as a reliable tool for assessing concrete structures affected by ASR. Depending on the extent of ASR damage in concrete, loading levels up to 40% of the compressive strength may contribute to increasing internal damage during testing. Nevertheless, previous research found that no additional damage was induced by the SDT. This confirmed the non-destructive character of the SDT making it valid to determine the compressive strength on the same test specimens following the SDT.

However, other research suggests that loading levels above 15% of the compressive strength could lead to load-induced damage in the first load cycle. The implication of the non-destructive character and the loading level of the SDT needs more attention, especially when testing anisotropically ASR-damaged concrete structures.

This paper thus presents a critical evaluation of the non-destructive character of the SDT by utilizing Acoustic Emission (AE) measurements. The SDT was used to evaluate an ASR affected concrete structure after 60 years in use. Several cores from cantilever slabs were extracted enabling damage assessment of the concrete structure in use. AE allowed to measure crack occurrence with a higher accuracy. Therefore, the critical load level could be more accurately identified using AE. The magnitude of enhancing internal damage during the SDT is related to the extent of ASR. From this study it can be concluded that the non-destructive character of the stiffness damage test depends the critical load level in relation to the internal degree of damage, which can be determined by means of Acoustic Emission.

Keywords: Alkali-Silica reaction · Stiffness damage test · Non-destructive testing · Acoustic emission · Damage assessment

L. F. M. Sanchez and C. Trottier (Eds.): ICAAR 2024, RILEM Bookseries 50, pp. 3–10, 2024.
https://doi.org/10.1007/978-3-031-59349-9_1

1 Introduction

To maintain ageing concrete structures affected by alkali-silica reaction (ASR), reliable diagnosing and damage assessment methods should be employed [1, 2]. For durability and service life prediction of concrete structures it is important to establish the relationship between ASR-induced cracking and loss of structural strength. When evaluating structural properties, only limited number of cores may be extracted from any structure. It is desirable that deteriorated strain-stress relationships could be determined without damaging the specimen, after which the core could be re-used to measure other parameters affected by ASR. Considering these requirements, the Stiffness Damage Test (SDT) was developed in the early 1990's by Chrisp et al. [3].

The initial test procedure and an early iteration were performed using a fixed load of 5.0 [3] or 10.0 MPa [4], respectively. Over the years the SDT has evolved and numerous parameters have been studied, such as the loading level and suitable output parameters for damage assessment [5, 6]. Earlier research found that no significant additional damage was induced by the SDT when evaluating the test specimens using a semi-quantitative petrographic method, Damage Rating Index (DRI) and Ultrasound Pulse Velocity (UPV) [6]. Hereafter, the SDT has been adopted into a multi-level approach for assessing restrained and unrestrained ASR-affected concrete structures [7–10].

Nevertheless, the non-destructive character and the loading level of this test is not uncontroversial and whether the maximum load used in the SDT should be reduced for restrained ASR affected concrete needs further research [11].

Therefore, this study attempts to give a new insight into the effect of the loading sequence and applied load on the test specimen during the stiffness damage test. The use of Acoustic Emission (AE) allows the researchers to identify the moment of inducing additional cracking in the test specimen, hence the limit level for which the test should be considered truly non-destructive.

2 Experimental Program

2.1 Materials and Sample Preparation

This paper presents the damage assessment of an ASR-affected post-tensioned concrete viaduct by evaluating several extracted cores using the SDT. As per the construction records, the viaduct was built in the 1960s using river dredged aggregates containing chert, approximately 350 kg/m^3 Ordinary Portland Cement and a concrete design strength of 30 MPa. The load bearing construction of the viaduct comprises of columns with a cantilever slab on top on which prestressed beam elements are placed. ASR was diagnosed at the bottom side of the slabs. Visual inspection of the viaduct suggests that the slabs show various degrees of damage. To quantify the degree of damage, cores of 100 mm in diameter were extracted in the vertical direction (Z) from different slabs with a length of 400 mm. It should be noted that the structural element was post-tensioned in the X and Y-direction. Therefore, the cores were taken in the least restrained direction. The extracted cores were wrapped in wet cloths and cling film and transported to the laboratory. The outer 50 mm of the extracted cores was discarded and the remaining part of the cores were used to obtain Ø100 × 200 mm test samples. Seven Ø100 × 200 mm samples were selected for evaluating the damage by means of the SDT.

2.2 Methodology

Stiffness Damage Test

Prior to testing, all samples were preconditioned for 48 h in a moist curing room at 20 °C, as proposed by Sanchez et al. [5]. Additionally, both ends of the concrete cores were flattened and ground by mechanical grinding.

The SDT was performed in a load-controlled manner using a hydraulic actuator with a maximum load of 1500 kN. It was decided to limit the maximum loading level to 10 MPa, as prescribed by [12]. First, an initial stress of 0.50 MPa was applied on the sample, afterwards the samples were loaded with a loading rate of 0.10 MPa/s until 10.0 MPa. After reaching the maximum applied stress, the sample was unloaded at a similar rate of 0.10 MPa/s until 0.5 MPa was reached. The full loading sequence of the SDT consisted of five loading-unloading cycles.

Four linear variable differential transformers (LVDTs) were circumferentially and centrally placed over a length of 100 mm and used to measure the vertical strain.

Parameters such as the Hysteresis Area (HA, in J/m^3), the area of the hysteresis loops averaged over the last four cycles and the chord loading stiffness (E_c, in GPa), the slope of the loading curve are evaluated and adopted from Chrisp et al. [3]. Additionally, parameters suggested by Sanchez et al. [6] such as the average secant stiffness (E_{SDT}, in GPa) of the unloading curves from the second and third load cycle, the ratio of dissipated energy to the total energy implemented in the system (SDI) and the plastic deformation accumulated during the SDT over the total deformation measured in the maximum load in the last loading cycle (PDI) were also measured.

Acoustic Emission

One wideband differential (WD) AE sensor (Mistras Group, Inc) was installed on the specimen surface (glued by hot melt adhesive) to record the AE signals during the entire cyclic test (Fig. 1). The operating frequency range of the used WD sensor was 100–900 kHz. The acquisition of AE signals was conducted using a 32-channel Micro-II

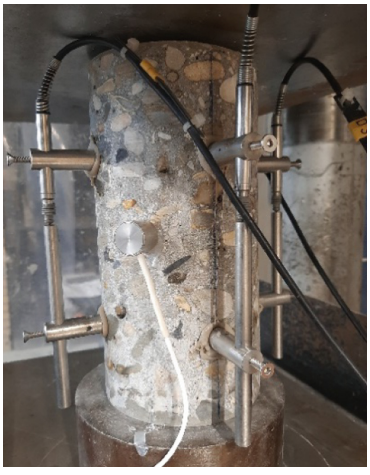

Fig. 1. Placement of the LVDT's and AE-sensor for measurements during the SDT.

Express Digital AE system (Mistras Group, Inc). The threshold and sampling rate for AE acquisition were initialized as 45 dB and 5 MHz, respectively. The hit definition parameters peak definition time (PDT), hit definition time (HDT) and hit lockout time (HLT) were set as 300, 600 and 1000 us, respectively. A band pass filter from 20 kHz to 1 MHz was used for the AE sensor. Pencil-leak break tests were conducted for each sensor before main tests to assure sensor sensitivity and the proper settings of AE monitoring system. Waveforms of the received AE sensors were then saved for further analysis.

3 Results and Discussion

Figure 2 shows stress-strain curves obtained during the stiffness damage test, on the test samples from the extracted cores, for two distinct degrees of damage due to ASR. Figure 2a shows a stress-strain curve that presents a low degree of damage, which was labelled as such based on the relatively higher slope of the loading and unloading cycles, representing the elastic modulus. Additionally, there was less dissipated energy (hysteresis area underneath the curve) and plastic deformation observed compared to Fig. 2b. A higher degree of damage was observed in samples represented by Fig. 2b. The slope of the first loading sequence and the slopes of the unloading sequences were significantly lower than that observed in Fig. 2a. For further analysis the samples with a lower damage degree were classified as Class I and the once with a higher degree of damage as Class II. Furthermore, the determined parameter values, as described in Sect. 2.2, from the obtained stress-strain curves were presented in Table 1.

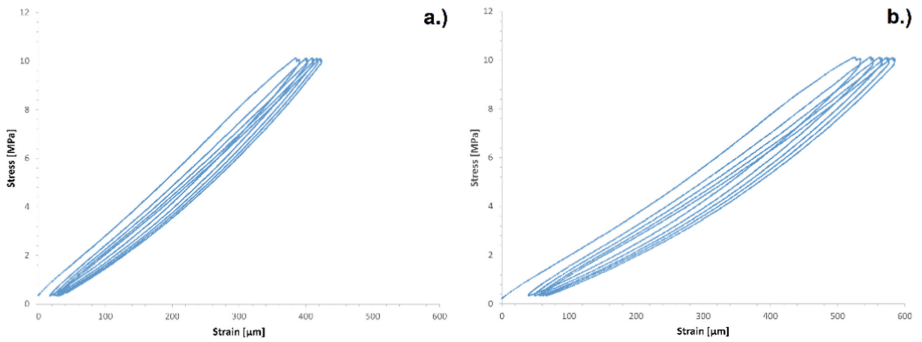

Fig. 2. Stress-strain curves from the SDT with different distinct damage degrees due to ASR a) low degree of damage b) high degree of damage.

E_c and E_{SDT} from Class II samples were 20–25% lower in comparison to Class I (Table 1). Furthermore, there was a clear increase in HA, PDI and SDI as also was observed from Fig. 2. The coefficient of variation of the Class II parameters were considerably higher than that of Class I. This was due to the classification of the test samples with a higher degree of damage. Nevertheless, for the following analysis of the non-destructive character of the SDT, it was found that multiple damage degrees could be grouped together.

Table 1. Test results from the stiffness damage test, as classified in 2 distinct groups.

		E_c [GPa]	E_{SDT} [GPa]	HA [J/m^3]	PDI [−]	SDI [−]
Class I (3 samples)	mean	24.3	24.3	221.9	0.01	0.12
	Std Dev	0.8	0.7	22.0	0.00	0.01
	CoV[a]	3.1	3.0	9.9	17.49	8.32
Class II (4 samples)	mean	18.0	19.4	415.8	0.12	0.19
	Std Dev	1.2	1.0	111.4	0.07	0.04
	CoV[a]	6.6	5.3	26.8	53.16	22.91

[a]Coefficient of variation

During the loading-unloading sequences of the SDT, AE signals were recorded which were assumed to arise from tensile cracking as well as the friction between the crack faces [13]. Frequency is a key AE-parameter to characterize the source of rupture and can be used to infer to the internal crack development and progressive damage within a sample. By plotting the loading-unloading cycles of the SDT in time in relation to the peak frequency obtained from the AE-measurements, clear zonal distribution of peak frequency signals was observed [14, 15]. The peak frequency signals were divided into three separate frequency bands. Frequency band I were the signals lower than 70 kHz and represented friction. Signals with a peak frequency higher than 70 kHz were identified as tensile cracking [13]. Small scale fracturing within the sample was marked by high frequency signals, band III [14]. For frequency band II there is no clear description for the relation between peak frequency and induced damage. It might be closely related to the closure of cracks and minor crack propagation, but further research is required for understanding the source of this signal.

To analyse the variation in peak frequency signals during the SDT for samples with different internal degrees of damage, the distribution of the three peak frequency bands were expressed as a percentage of the total number of signals and plotted in Fig. 4. The results show that while performing the SDT on a sample with a higher damage degree (i.e. class II), significantly more high frequency signals were recorded, indicating that additional internal damage was induced. On the other hand, in samples with a lower degree of damage (i.e. class I), mainly signals in the middle frequency band occurred, indicating the process of crack closure. Therefore, it can be found that samples with a higher degree of damage would exhibit enhanced internal damage, through the SDT when applying a too high of a loading level.

Sanchez et al. have already discussed that the extent of damaging effect during loading depends on both the extent of the ASR-reaction as well as the scale of the applied techniques for evaluation [6]. It is very likely that AE indicated the occurrence of micro-cracking, which do not necessarily lead to a reduction in mechanical performance. Nevertheless, for better understanding the stress-strain behaviour of ASR-affected concrete, knowledge on the stiffness reduction, nonlinear stress-strain behaviour and dissipated

energy is required [11]. The stiffness damage test has this potential, however, the stress-strain relation and the evaluated parameters should only represent internal damage due to ASR. It is therefore imperative that the loading level does not necessarily induce additional damage during the test. If there was damage induced during the test, then there should be an increase in dissipated energy, increase in plastic deformation and decrease in modulus of elasticity which then is incorrectly associated with ASR. Therefore, AE could be used to establish the critical loading level, for which no signals in frequency band III occur (Fig. 3).

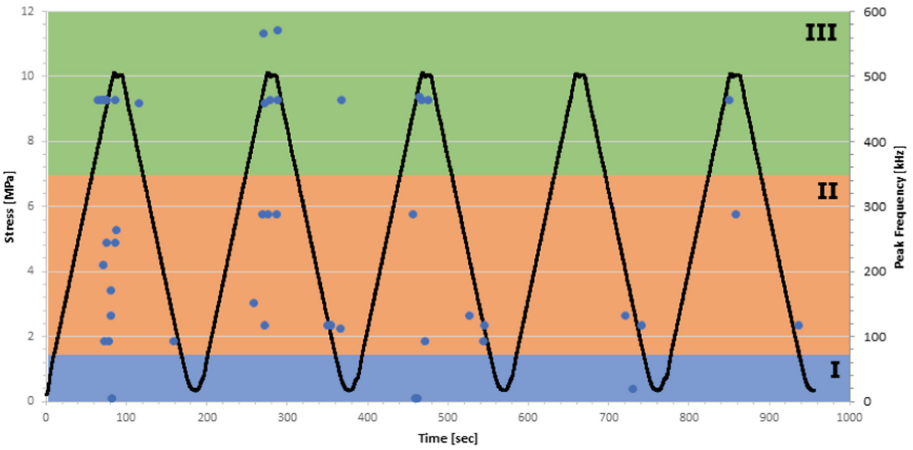

Fig. 3. Peak frequency distribution in relation to time and the loading sequence of the SDT.

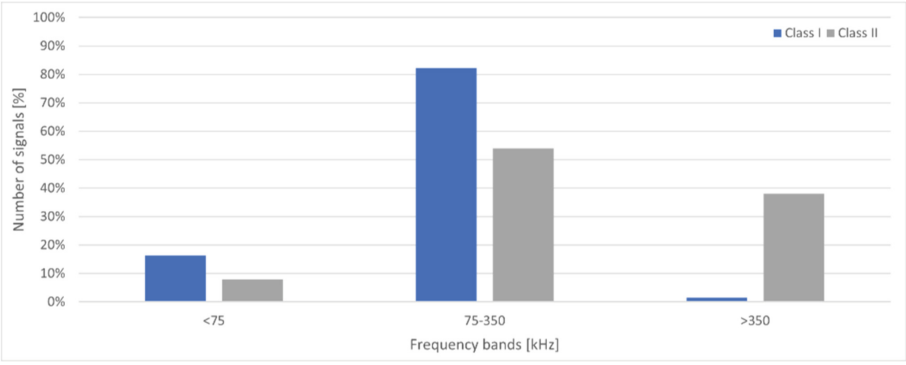

Fig. 4. Variation in the three frequency bands by average number of signals [%] during the SDT samples with a different damage degree.

4 Concluding Remarks

From this study it can be concluded that the non-destructive character of the stiffness damage test depends the critical load level in relation to the internal degree of damage. For a higher degree of internal damage, the loading level should be reduced, and should be considered depending on the internal damage degree rather than the concrete compressive strength.

For further research, a constitutive relation between internal damage induced by ASR and the critical loading level for the stiffness damage test should be established. The use of acoustic emission is a very useful tool to find the critical loading level for the stiffness damage test. Small scale cracking and crack propagation, indicated by high frequency signals in frequency band III, should be avoided and the loading level must be tailored to this. Furthermore, it should be verified whether these high frequency signals indeed lead to increase of internal cracking and what is the extent of these cracks.

References

1. Swamy, R.N.: Assessment and rehabilitation of AAR-affected structures. Cem. Concr. Compos. **19**, 427–440 (1997)
2. Fournier, B., Bérubé, M.A.: Alkali-aggregate reaction in concrete: a review of basic concepts and engineering implications. J. Civil Eng. **27**, 167–191 (2011). https://doi.org/10.1139/L99-072
3. Chrisp, T.M., Waldron, P., Wood, J.G.M.: Development of a non-destructive test to quantify damage in deteriorated concrete. Mag. Concr. Res. **45**, 247–256 (1993). https://doi.org/10.1680/MACR.1993.45.165.247
4. Smaoui, N., Bérubé, M.A., Fournier, B., Bissonnette, B., Durand, B.: Evaluation of the expansion attained to date by concrete affected by alkali–silica reaction. Part I: experimental study. Can. J. Civil Eng. **31**, 826–845 (2011). https://doi.org/10.1139/L04-051
5. Sanchez, L.F.M., Fournier, B., Jolin, M., Bastien, J.: Evaluation of the Stiffness Damage Test (SDT) as a tool for assessing damage in concrete due to alkali-silica reaction (ASR): input parameters and variability of the test responses. Constr. Build. Mater. **77**, 20–32 (2015). https://doi.org/10.1016/j.conbuildmat.2014.11.071
6. Sanchez, L.F.M., Fournier, B., Jolin, M., Bastien, J.: Evaluation of the stiffness damage test (SDT) as a tool for assessing damage in concrete due to ASR: test loading and output responses for concretes incorporating fine or coarse reactive aggregates. Cem. Concr. Res. **56**, 213–229 (2014). https://doi.org/10.1016/j.cemconres.2013.11.003
7. Sanchez, L.F.M., Drimalas, T., Fournier, B., Mitchell, D., Bastien, J.: Comprehensive damage assessment in concrete affected by different internal swelling reaction (ISR) mechanisms. Cem. Concr. Res. **107**, 284–303 (2018). https://doi.org/10.1016/J.CEMCONRES.2018.02.017
8. Sanchez, L.F.M., Fournier, B., Jolin, M., Mitchell, D., Bastien, J.: Overall assessment of Alkali-Aggregate Reaction (AAR) in concretes presenting different strengths and incorporating a wide range of reactive aggregate types and natures. Cem. Concr. Res. **93**, 17–31 (2017). https://doi.org/10.1016/J.CEMCONRES.2016.12.001
9. Sanchez, L.F.M., Fournier, B., Mitchell, D., Bastien, J.: Condition assessment of an ASR-affected overpass after nearly 50 years in service. Constr. Build. Mater. **236**, 117554 (2020). https://doi.org/10.1016/J.CONBUILDMAT.2019.117554

10. Zahedi, A., Trottier, C., Sanchez, L., Noël, M.: Evaluation of the induced mechanical deterioration of alkali-silica reaction affected concrete under distinct confinement conditions through the Stiffness Damage Test. Cem. Concr. Compos. **126**, 104343 (2022). https://doi.org/10.1016/J.CEMCONCOMP.2021.104343
11. Kongshaug, S.S., Oseland, O., Kanstad, T., Hendriks, M.A.N., Rodum, E., Markeset, G.: Experimental investigation of ASR-affected concrete – the influence of uniaxial loading on the evolution of mechanical properties, expansion and damage indices. Constr. Build. Mater. **245**, 118384 (2020). https://doi.org/10.1016/J.CONBUILDMAT.2020.118384
12. Smaoui, N., Fournier, B., Bérubé, M.A., Bissonnette, B., Durand, B.: Evaluation of the expansion attained to date by concrete affected by alkali-silica reaction. Part II: application to nonreinforced concrete specimens exposed outside. Can. J. Civil Eng. **31**, 997–1011 (2004). https://doi.org/10.1139/L04-074
13. Zhang, F., Yang, Y., Fennis, S.A.A.M., Hendriks, M.A.N.: Developing a new acoustic emission source classification criterion for concrete structures based on signal parameters. Constr. Build. Mater. **318**, 126163 (2022). https://doi.org/10.1016/J.CONBUILDMAT.2021.126163
14. Liu, X., Liu, Z., Li, X., Gong, F., Du, K.: Experimental study on the effect of strain rate on rock acoustic emission characteristics. Int. J. Rock Mech. Min. Sci. **133**, 104420 (2020). https://doi.org/10.1016/J.IJRMMS.2020.104420
15. Song, X., Yu, X., Zhao, W., Yang, F., Shi, J., Yalçınkaya, Ç.: Progressive damage process and destabilization precursor recognition of sulfate tailing-cemented paste backfill based on acoustic emission. Powder Technol. **430**, 119047 (2023). https://doi.org/10.1016/J.POWTEC.2023.119047